

THERMAL STABILITY OF INCONEL ALLOY 783 AT 593°C AND 704°C

Sarwan K. Mannan, Gaylord D. Smith, Shailesh J. Patel
Special Metals Corporation, Huntington, WV, USA

Key Words: INCONEL alloy 783, Thermal Stability, Dimensional Stability, Microstructure, Low CTE, Tensile Properties

Abstract

INCONEL^{*} alloy 783 is a low co-efficient of thermal expansion (CTE) superalloy. It is designed for high strength, good oxidation resistance, and higher temperature capability as compared to 900-series alloys. In this study, commercially produced alloy 783 was isothermally exposed at 593°C for up to 12,000h and at 704°C for up to 4,000h. This was followed by high temperature tensile testing and microstructural analysis. INCOLOY^{*} alloy 909 was also isothermally exposed and tested under similar conditions to compare thermal stability. Isothermal exposure at 593°C resulted in significant decrease in strength for alloy 909, whereas the strength of alloy 783 was unaffected with this exposure. High temperature elongation of alloy 783 degraded to mid-teens with the initial 1,000h exposure at 593°C and thereafter remained essentially constant for up to 12,000h exposure. On 704°C exposure, both the alloys lost significant strength, however, the loss of strength was more pronounced for alloy 909.

Introduction

Materials used in gas turbines must have good high temperature microstructural and dimensional stability. To avoid degradation in strength due to overaging, precipitation strengthened superalloys are used at intermediate temperatures where phase transformations are rather sluggish. Since evaluation of intermediate temperature stability requires prolonged isothermal exposure and extensive testing, the data on intermediate temperature stability is scarce.

Low CTE alloys are used in selected gas turbine components due to their tighter clearance control, which enhances engine efficiency. Properties of low CTE 900-series alloys: 903, 907, and 909 are presented in a review publication [1]. These alloys are prone to severe stress assisted grain boundary oxidation (SAGBO) due to their negligible Cr content. Further, due to metallurgical instability, their maximum operating temperature is limited to approximately 600°C. Alloy 783 is designed to overcome these limitations of 900-series alloys.

Alloy 783 is a three-phase material. It has a specially designed austenitic matrix for good hot/cold workability, fine Ni₃Al-type gamma prime for high strength, and inter- and intra-granular NiAl-type beta phase for good SAGBO and general oxidation / corrosion resistance [2,3]. This study presents a comparative

thermal stability of alloys 783 and 909 at 593°C and 704°C. The materials were high temperature tensile tested following extended high exposure. Microstructural analyses were done to understand the observed change in properties

Experimental Procedure

Commercially hot-finished 19 mm rod of alloy 783 was lab annealed at 1121°C for 1h and water quenched. This was followed by heat treatment at 843°C for 4h and air cool. Then, these samples were two step aged: 718°C/8h, furnace cooled at 56°C/h to 621°C/8h, air cooled. Following these heat treatments, rough-machined samples were isothermally exposed at 593°C for times up to 12,000 hours, machined, and tensile tested at room temperature and at 649°C. A 101.6 mm commercially produced rod was used to repeat selected isothermal exposures at 593°C. Samples from this bar were also exposed at 704°C for times up to 4,000 hours, machined, and tensile tested at room temperature and at 704°C. To study the effect of environment, a set of samples were tested at 649°C in vacuum following 593°C isothermal exposure in air. The vacuum was of the order of 5×10^{-6} Torr.

To compare thermal stability of alloy 783 with a well-known low CTE alloy, specimens from a lab rolled 16.9 mm INCOLOY alloy 909 rod were isothermally exposed at 593°C and 704°C and tested under similar conditions. Alloy 909 was annealed at 982°C for 1h, air-cooled, and two step aged similar to alloy 783 as mentioned above. Chemical composition of the materials is shown in Table 1. Grain size was determined by comparison method. Grain size of alloys 783 and 909 were ASTM 9 and 9.5 respectively.

Annealed plus aged alloy 783 was isothermally exposed at 593°C to measure dimensional stability. Shrinkage was in-situ monitored at 593°C using a single push rod dilatometer by means of linearly variable differential transducers. Strain resolution was better than $\pm 0.001\%$. The specimens were thermally equilibrated at the test temperature for about 30 minutes prior to monitoring dimensional changes. Long term stability of this set up was found to be better than 0.002% using a platinum standard. Since the testing was done in air, some oxidation of specimens occurred. However, the thickness of any oxide film was negligible as compared to the measured length change.

Swab etching with Kalling's reagent containing 6 gm CuCl₂, 100 ml HCl, 100 ml H₂O, and 100 ml CH₃OH was used to reveal the microstructure. To prepare samples for transmission electron microscope (TEM), 400-500 μm thick foils were cut with a precision saw. The 3 mm discs were mechanically punched from the foils and ground to 150-200 μm . The discs were then electrolytically polished by a twin jet thinning apparatus using a solution of 10% perchloric acid in methanol at 28V and at -50°C . Thin foils were examined with Phillips EM400 TEM.

* INCONEL and INCOLOY are the registered trademarks of the Special Metals Family of Companies

Table I. Chemical Compositions of the Tested Alloys 783 and 909, Weight %.

Alloy	Ni	Fe	Cr	Co	Nb	Al	Ti	C	Si
783 (101.6 mm)	28.0	25.0	3.2	34.9	3.0	5.39	0.20	0.008	0.06
783 (19 mm)	28.0	24.9	3.3	35.1	3.0	5.33	0.20	0.008	0.06
909	38.3	41.4	0.1	12.9	5.10	0.05	1.56	0.005	0.42

Results

Tensile Properties

Table II shows that room temperature tensile properties of alloy 783 are essentially unaffected by isothermal exposure at 593°C of up to 10,000 hours. Table III shows that 593°C exposure did not affect 649°C yield strength, however, % elongation dropped from thirties to mid-teens with initial 1000h exposure and thereafter remained essentially constant for up to 12,000h exposure. Tensile properties of as-produced and 593°C exposed specimens tested at 649°C in vacuum are shown in Table IV. These tests do not show any degradation in elongation on isothermal exposure. It should be mentioned that the air tested specimens were rough ground whereas the vacuum tested specimens were low-pressure ground. Therefore, the difference in elongation value is most likely due to difference in environment and surface roughness.

Table II. Room temperature tensile properties of 19 mm alloy 783 rod following 593°C exposure. Yield strength, tensile strength, elongation, and reduction of area are denoted by YS, UTS, El, and RA Respectively.

Exposure Time	YS, MPa	UTS, MPa	% El	% RA
0	850	1277	21	40
	847	1275	21	43
1000h	885	1311	19	41
	850	1261	19	39
2000	881	1296	20	39
	871	1291	20	40
4000h	894	1304	20	24
	892	1309	19	24
8000h	885	1294	19	44
	876	1262	19	40

To obtain design data and also to repeat some of the single data points, a set of five samples were tensile tested at 649°C in as-produced condition and after isothermal exposure at 593°C for 3000h, 6000h, 7000h, and 8000h. Data in Table V shows that the yield strength at 649°C is not affected by exposure of up to 8,000h. As-produced elongation was 25 to 31%. There is quite a bit of scatter for elongation of exposed specimens. On 3000h exposure, the % elongation remains in twenties. On 6000h exposure, there were four tests with % elongation in twenties and one test in teens. On 7000h exposure, there were two tests with elongation in the teens and for 8000h exposure, there were three tests with elongation in the teens. The lowest elongation obtained in this test matrix was 12%. Yield strength and elongation plots at

649°C with 593°C exposure are shown in Figure 1. It should be mentioned that this test matrix was conducted on mill annealed plus aged 101.6 mm rod. Mill annealing and aging conditions were same as that of lab samples. The proceeding test matrix was conducted on 19 mm rod, hot finished in the mill and annealed and aged in the lab.

Table III. 649°C Tensile properties of 19 mm alloy 783 rod following 593°C exposure. Yield strength, tensile strength, elongation, and reduction of area are denoted by YS, UTS, El, and RA respectively.

Exposure Time	YS, MPa	UTS, MPa	% El	% RA
0	710	983	37	44
	708	985	39	62
1000h	733	992	15	22
	700	976	17	21
2000h	721	1008	34	66
	727	1002	19	21
3000h	728	1006	15	21
	741	1016	15	19
4000h	714	986	18	26
	740	1043	20	30
5000h	752	1036	22	34
	735	1011	14	19
6000h	734	1010	12	19
7000h	734	1023	13	18
8000h	743	996	8	12
9000h	742	1027	19	28
	743	1043	21	31.4
10,000h	721	1018	19	29
12,000h	737	1023	25	37

Table IV. 649°C Tensile properties of 19 mm alloy 783 rod following 593°C exposure. Yield strength, tensile strength, elongation, and reduction of area are denoted by YS, UTS, El, and RA respectively. Test blanks were exposed and the samples were tested in vacuum after machining.

Exposure Time	YS, MPa	UTS, MPa	% El	% RA
0	717	1041	26	63
	731	1027	26	65
1000h	738	1076	32	61
	751	1089	31	68
5000h	793	1131	27	57
	765	1083	39	69
10,000h	752	1021	33	68

Table V. 649°C Tensile properties of 593°C exposed alloy 783. These samples were obtained from a fully mill processed 101.6 mm rod. Yield strength, tensile strength, elongation, and reduction of area are denoted by YS, UTS, El, and RA respectively.

Exposure Time	YS, MPa	UTS, MPa	% El	% RA
0	713	950	25	34
	774	963	27	35
	771	955	31	43
	779	966	31	54
3000h	736	970	25	35
	749	983	21	23
	806	1027	29	48
	827	1032	27	49
	725	983	26	33
6000h	792	989	24	31
	756	994	28	41
	757	994	13	28
	734	984	27	41
7000h	802	1006	22	31
	738	975	34	64
	795	1024	13	14
	803	992	32	69
	727	988	27	51
8000h	804	1046	15	22
	757	994	19	24
	739	985	13	22
	744	983	25	36
	777	971	12	16
	748	1002	24	40

Table VI. 649°C Tensile properties of alloy 909 following 593°C exposure. Yield strength, tensile strength, elongation, and reduction of area are denoted by YS, UTS, El, and RA respectively. The Values are the averages of duplicate tests.

Exposure time	YS, MPa	UTS, MPa	% El	% RA
0	819	972	26	54
1000h	846	972	19	45
2000h	833	986	19	66
4000h	773	931	23	62
6000h	700	890	23	61
8000h	628	821	27	69
10,000h	561	783	29	71
12,000h	536	756	29	73

Table VI shows 649°C tensile properties of alloy 909 following 593°C exposure. Yield strength increases slightly with initial 1000h and 2000h exposures and then on 4000h onwards, the yield strength decreases with increase in exposure time. On exposure of 12,000h at 593°C, the alloy loses 35% of its starting strength. Yield strength variations of alloys 783 and 909 at 649°C following 593°C exposure are shown in Figure 2.

Tables VII and VIII show room temperature and 704°C tensile properties of alloy 783 following 704°C exposure. Yield strength decreases with increase in exposure time. Room temperature elongation is unaffected with exposure time. However, 704°C elongation and reduction of area are slightly increased with increase in exposure time. Tensile properties of alloy 909 at 704°C following 704°C exposure is shown in Table IX. As expected based on 593°C exposure data, alloy 909 also show degradation in strength. However, the decrease in yield strength for alloy 909 is more pronounced than alloy 783. After 4000h exposure at 704°C, the drop in yield strength for alloys 783 and 909 were 33% and 51%, respectively. Yield strength variation of alloys 783 and 909 at 704°C on 704°C exposure are shown in Figure 3.

Table VII. Room temperature tensile properties of alloy 783 following 704°C exposure. Yield strength, tensile strength, elongation, and reduction of area are denoted by YS, UTS, El, and RA respectively. The data is an average of duplicate tests.

Exposure Time	YS, MPa	UTS, MPa	% El	% RA
As-produced	885	1293	18.7	36.5
100h	872	1227	17.9	40.0
500h	847	1215	18.2	40.5
1000h	740	1152	18.6	46.2
2000h	719	1133	17.1	35.2
4000h	709	1128	17.7	33.6

Table VIII. 704°C tensile properties of alloy 783 following 704°C exposure. Yield strength, tensile strength, elongation, and reduction of area are denoted by YS, UTS, El, and RA respectively. The data is an average of two tests.

Exposure Time	YS, MPa	UTS, MPa	% El	% RA
As-produced	650	816	41.4	73
100h	628	773	38.5	75.3
500h	556	740	41.1	77.5
1000h	516	689	44.6	79.9
2000h	455	656	44.8	80.5
4000h	433	624	47.0	83.9

Table IX. 704°C tensile properties of alloy 909 following 704°C exposure. Yield strength, tensile strength, elongation, and reduction of area are denoted by YS, UTS, El, and RA respectively. The data is average of two tests.

exposure time, h	YS, MPa	UTS, MPa	% El	% RA
As-produced	676	776	35	72
100h	491	625	51	92
500h	383	556	40	94
1000h	377	530	49	95
2000h	330	510	42	89
4000h	332	476	41	95

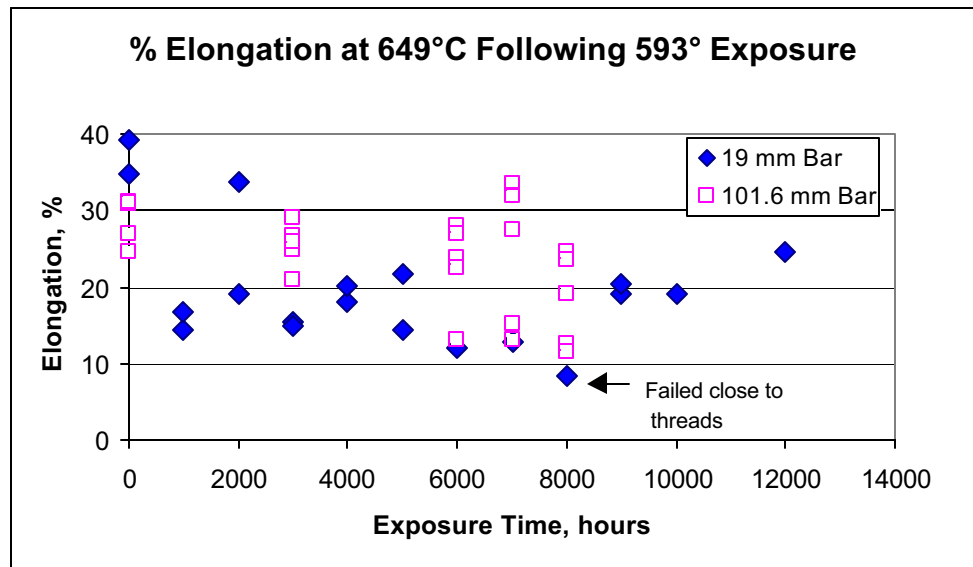
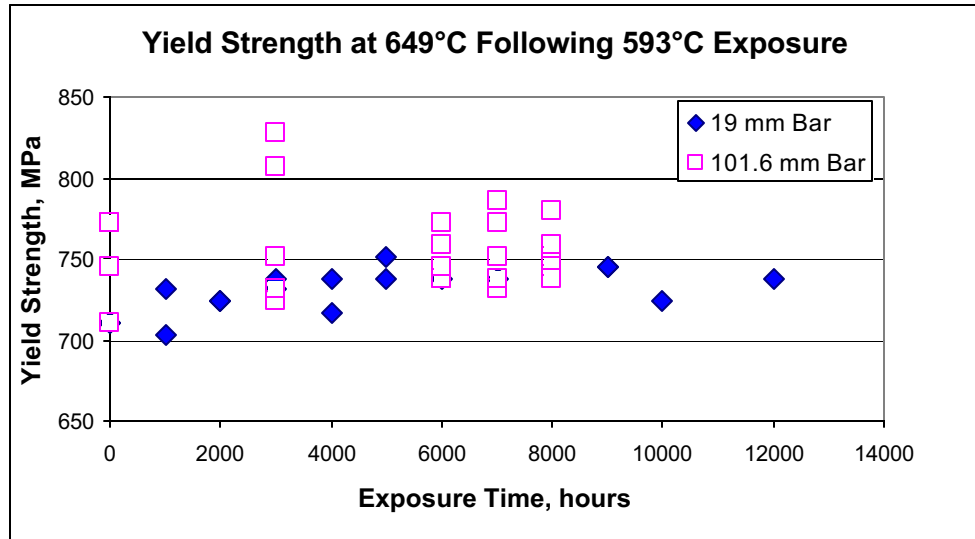


Figure 1. 649°C Tensile Properties of Alloy 783 Following Isothermal Exposure at 593°C. Upper Graph is Yield Strength and the Lower Graph is Percentage Elongation.

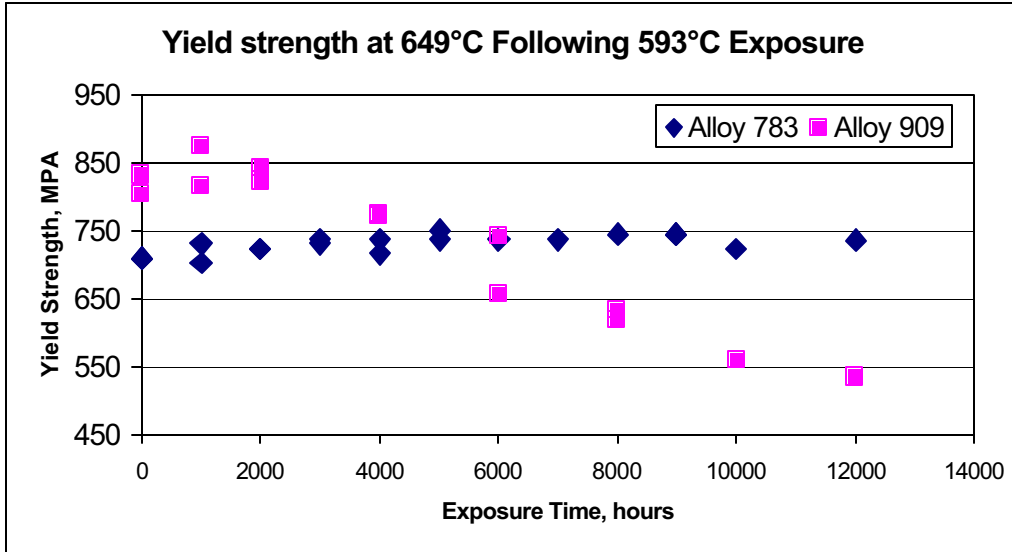


Figure 2. 649°C Yield Strength of Alloys 783 and 909 Following Isothermal at 593°C. Higher Temperature Capability of Alloy 783 is Revealed.

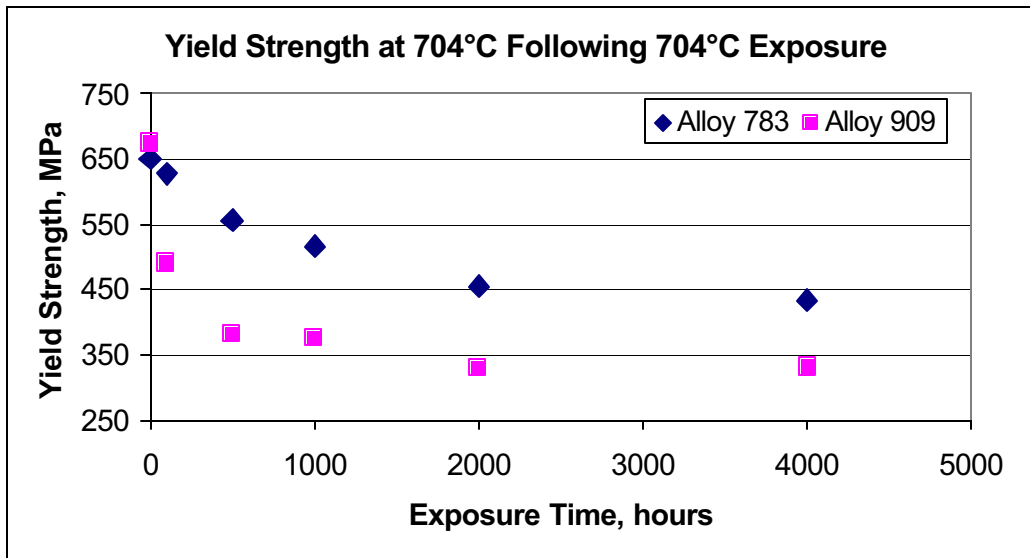


Figure 3. 704°C Yield Strength of Alloys 783 and 909 Following 704°C Exposure.

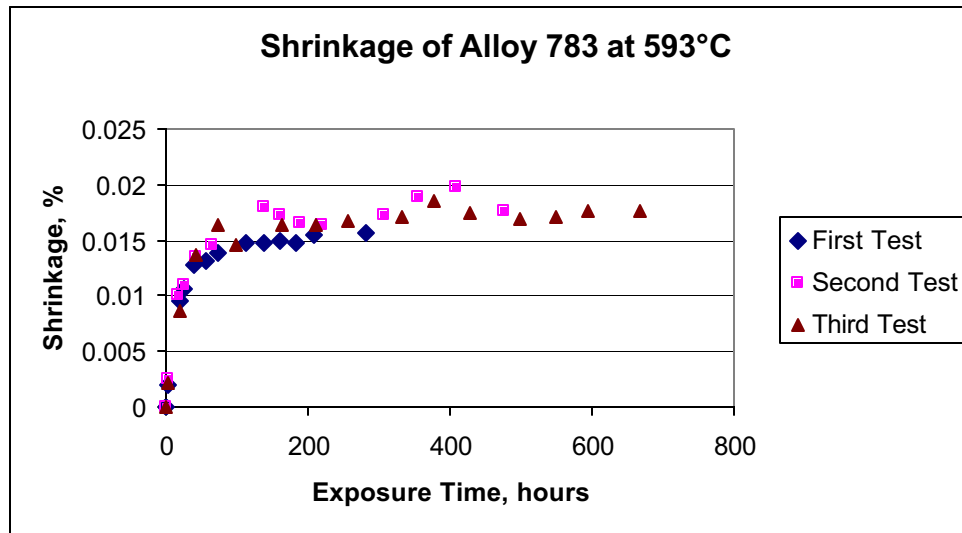


Figure 4. Shrinkage of Alloy 783 on Isothermal Exposure at 593°C. This Change in Dimensions was In-situ Monitored at 593°C with a Dilatometer.

Dimensional Stability

Figure 4 shows shrinkage of annealed plus aged alloy 783 on prolonged isothermal exposure at 593°C. Three independent test results are plotted. The material tends to shrink fairly rapidly upon exposure and after about 200h exposure, the shrinkage appears to reach saturation value. The total shrinkage after up to 600h exposure is approximately 0.02%. This shrinkage is likely to be related to additional aging on high temperature exposure. This type of dimensional stability data at the application temperature is very valuable for design consideration. A more detailed work on dimensional stability on isothermal exposure and stress relaxation behavior for alloy 783 is published elsewhere [4].

Microstructural Analysis

Figure 5 shows an optical photograph of annealed plus aged alloy 783. Most of the particles shown in this figure are NiAl-type beta precipitates. Rod-like inter-granular beta is primarily formed on 843°C/4h aging treatment mentioned in the experimental section. This heat treatment is commonly referred to as “beta-age”. In addition to these inter-granular rod-like beta phase, Figure 5 also contains geometric / globular inter- and intra-granular beta particles. These precipitates are formed during thermo-mechanical processing and are not completely dissolved on annealing. The solvus temperature of beta phase is 1175°C and the annealing temperature of alloy 783 is 1121°C. Alloy 783 is forged, rolled, and annealed below the beta solvus temperature for grain refinement.

TEM analysis shows that annealed plus aged alloy 783 has a bimodal gamma prime distribution, Figure 6a. Large cuboidal particles are formed on beta aging and fine irregular particles are formed on two-step aging mentioned earlier. These fine gamma prime particles are responsible for high strength. Figure 6b shows

beta particles, cuboidal coarse gamma prime and irregular fine gamma prime. There is no coarse cuboidal gamma prime in the vicinity of beta particle. Large Al-rich beta particle presumably resulted in Al-depletion of the adjacent matrix inhibiting coarse gamma prime formation.

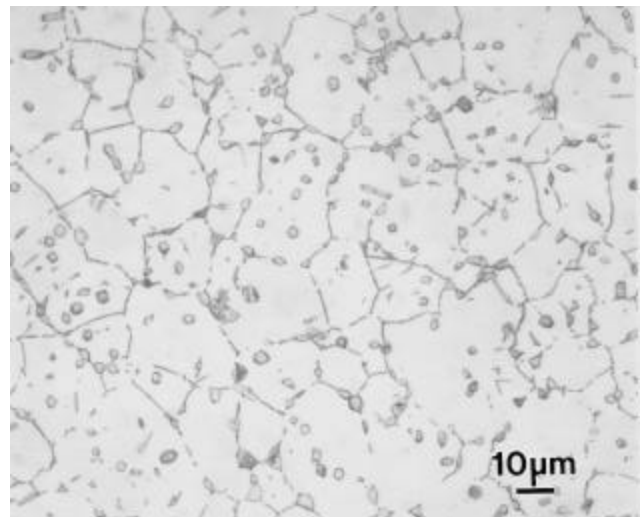
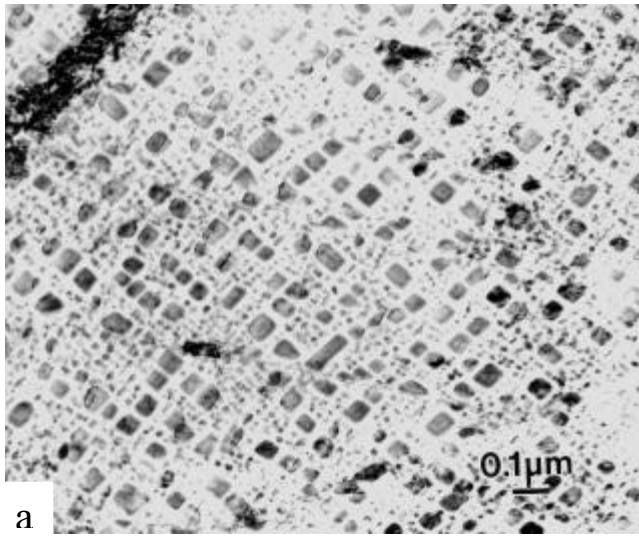
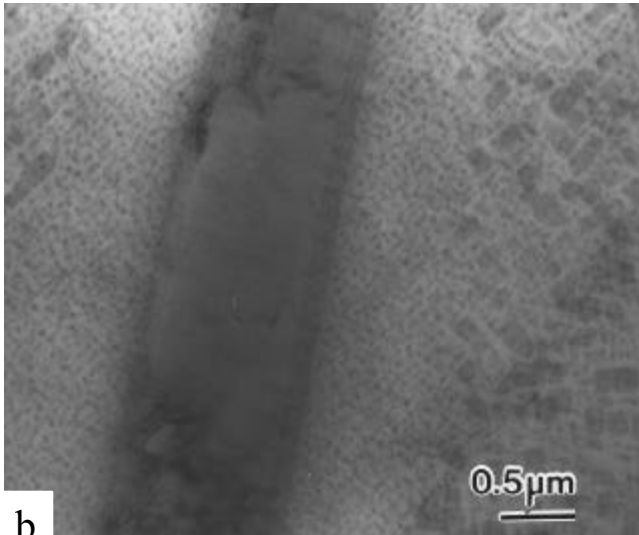


Figure 5. Optical Photograph of Annealed Plus Aged Alloy 783. Beta Phase Precipitates are Revealed.



a



b

Figure 6a & 6b. TEM Photographs of Annealed Plus Aged Alloy 783 Showing Bimodal Gamma Prime Distribution (6a) and Beta Phase (6b).

High magnification TEM photograph shows that beta phase in as-produced material is devoid of any internal precipitation, Figure 7. The specimen exposed at 593°C for 1000h contains some fine internal precipitates, Figure 8. High magnification TEM photograph reveals that beta phase in isothermally exposed material contains gamma prime precipitates, Figure 9. The microstructures of the specimens exposed at 593°C for 1000h and 8000h were similar.

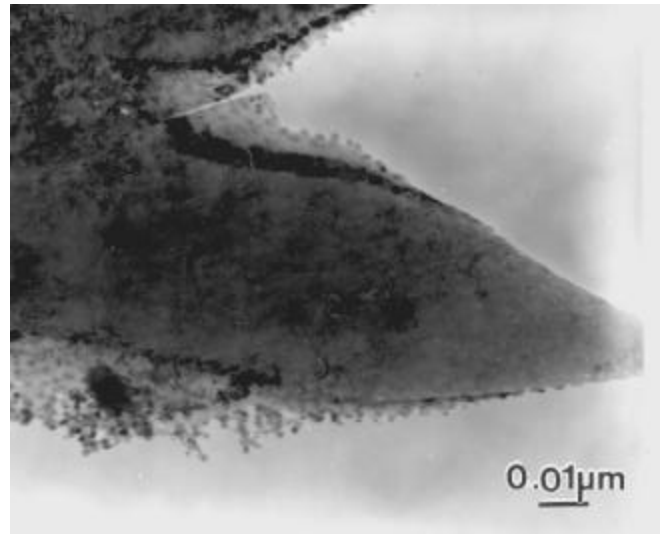


Figure 7. Transmission Electron Photomicrograph of As-produced Material Showing β Phase Completely Devoid of any Internal Precipitation.

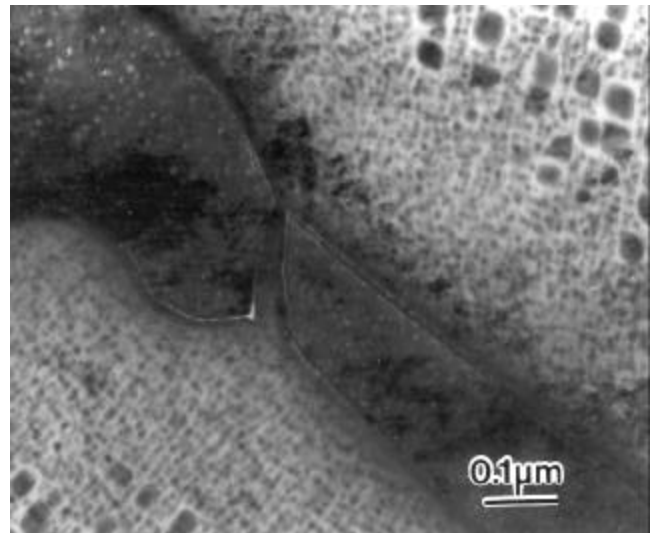


Figure 8. Transmission Electron Photograph of Alloy 783 Isothermally Exposed at 593°C for 1000h. Fine Precipitates Within Beta Phase are Revealed.

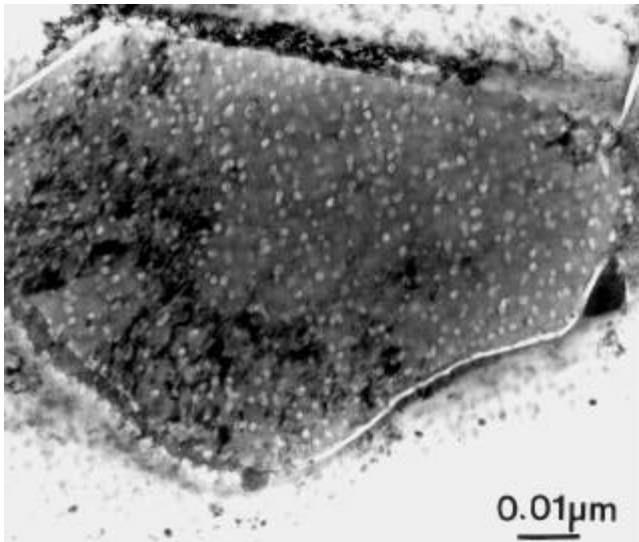


Figure 9. TEM Photograph of the Specimen Isothermally Exposed at 593°C for 1000 hours. Gamma Prime Precipitates Within Beta Phase are Revealed.

Discussion

Beta Phase Precipitates in Alloy 783

Beta phase is thought to be responsible for good stress rupture, static crack growth, corrosion resistance, and high temperature tensile properties of alloy 783 [5,6]. Since beta phase distribution is governed by thermo-mechanical processing, hot working conditions for direct-aged material was shown to have significant affect on fatigue crack propagation [7]. Studies have shown that inter-granular beta phase is essential for good time-dependent fatigue crack growth resistance [8,9]. Material without the presence of beta resulted in sustained loading crack growth whereas, beta-containing alloy 783 exhibited crack growth retardation and oxide induced crack closure.

In this study, TEM analysis confirmed that crystal structure of beta phase was ordered CsCl-type. The lattice parameter of beta phase was 0.287nm, which fits well with the reported literature [10]. Beta phase chemical composition was determined by SEM/EDX. It contained approximately 30%Ni, 24%Co, 15%Fe, and 31%Al by atom percentage. Since Co and Fe would occupy Ni lattice sites, the $(\text{NiCoFe})_{0.69}\text{Al}_{0.31}$ -type beta phase will be Ni-rich. Studies have shown that Ni-rich beta phase in NiAl system transforms to gamma prime, Ni_5Al_3 , and somewhat equiatomic NiAl [11,12]. Therefore, the presence of gamma prime on isothermal exposure at 593°C is not surprising. Dispersion strengthening and consequent decrease in ductility of beta phase is a plausible explanation of decrease in high temperature elongation of alloy 783 on isothermal exposure [13]. Time-dependent fatigue crack growth resistance of alloy 783 tested at 538°C and 650°C following isothermal exposure at 500°C for 3000h was slightly degraded as compared to as-produced alloy 783 [14]. However, the performance of alloy 783 was comparable to as-produced alloy 718 [14].

Degradation in Strength on Exposure

The results show that prolonged exposure at 593°C did not affect 650°C yield strength of alloy 783, whereas the yield strength of alloy 909 was significantly degraded. Further, on 704°C isothermal exposure, alloy 783 lost 33% of its starting strength whereas alloy 909 lost 51% on its starting strength. This clearly demonstrates that alloy 783 has higher temperature capability than alloy 909. Loss of strength in both the alloys is due to coarsening of gamma prime precipitates. Coarsening rate of gamma prime is thought to be related to coherency strain [15]. Increasing the Ti/Al ratio was found to increase coherency strain and the gamma prime coarsening rate of Ni-based superalloys [16,17]. Combination of low Ti and high Al in alloy 783 is specially designed to reduce coherency strain and improve high temperature capability over alloy 909, which has negligible Al and significant amount of Ti.

Conclusions

1. Isothermal exposure of up to 12,000 hours at 593°C did not affect high temperature yield strength of alloy 783. However, alloy 909 lost 35% of its starting yield strength under these testing conditions.
2. Multiple testing confirmed that isothermal exposure at 593°C decreased high temperature % elongation to mid-teens with the initial 1000h exposure and remained essentially constant thereafter for up to 12,000h exposure. This decrease in elongation appears to be related to the fine precipitation of gamma prime within the beta phase phase.
3. Isothermal exposure of up to 4,000h at 704°C decreased high temperature yield strength of alloys 909 and 783. The degradation in strength is more pronounced in alloy 909. Loss of strength on 704°C exposure is related to gamma prime coarsening. Published literature revealed that inferior thermal stability of alloy 909 is related to higher Ti/Al ratio, which is known to increase coherency strain and coarsening kinetics.
4. In-situ dilatometry showed that shrinkage in annealed plus aged alloy 783 on extended 593°C exposure is approximately 0.02%.

References

1. K. C. Russell and D. F. Smith, "A history of controlled, Low thermal Expansion Superalloys", Physical Metallurgy of Controlled Expansion Invar-Type Alloys, Edited by K. C. Russell and D. F. Smith, TMS, 1990, pp. 253-272.
2. K. A. Heck, D. F. Smith, M. A. Holderby, J. S. Smith, "Three Phase Controlled Expansion Superalloys with Oxidation Resistance", Superalloys 1992, Edited by S. D. Antolovich et al., TMS, 1992, pp. 217 – 226.
3. K. Heck, J. S. Smith, R. Smith, "INCONEL Alloy 783: An Oxidation Resistance, Low Expansion Superalloy for Gas Turbine Application", Journal of Engineering for Gas Turbine and Power, April 1998, Vol. 120, pp. 1-7.
4. M. G. Fahmann, A. A. Wereszczak, T. P. Kirkland, "Stress Relaxation Behavior and Dimensional Stability of INCONEL alloy 783", Materials Science & Engineering, Vol. A271, 1999, pp. 122-127.

5. J. S. Smith and K. A. Heck, "Development of a Low Thermal Expansion, Crack Growth Resistance Superalloy", Superalloys 1996, Edited by R. D. Kissinger et al., TMS, 1996, pp. 91-100.
6. E. C. Ott, J. R. Groh, S. K. Mannan, "Environmental Behavior of Low Thermal Expansion INCONEL alloy 783", To be published in Superalloys 2004.
7. L. Z. Ma, K. M. Chang, S. K. Mannan, S. J. Patel, "Effect of Thermomechanical Processing on Fatigue Crack Propagation in INCONEL alloy 783", Superalloys 2000, Edited by T. M. Pollock et al, TMS, 2000, pp. 601-608.
8. L. Z. Ma, K. M. Chang, S. K. Mannan, S. J. Patel, "Effect of NiAl-beta Precipitates on Fatigue Crack Propagation of INCONEL alloy 783 Under Time-Dependent Condition with Various Loads", *Scripta Materialia*, Vol. 48, 2003, pp. 551-557.
9. L. Z. Ma, K. M. Chang, S. K. Mannan, "Oxide-Induced Crack Closure: An Explanation for Abnormal Time-Dependent Fatigue Crack Propagation Behavior in INCONEL alloy 783", *Scripta Materialia*, Vol. 48, 2003, pp. 583-588.
10. A Taylor and B. J. Kagle, Compilers, Crystallographic Data on Metals and Alloy Structures, (New York: NY: Dover Publication, Inc, 1963), p. 27.
11. I. M. Robertson and C. M. Wayman, "Tweed Microstructures in Several NiAl Systems", *Philosophical Magazine*, Vol. 48, No. 3, 1983, pp. 443-467.
12. K. S. Kumar, S. K. Mannan, R. K. Viswanadham, "Fracture Toughness of NiAl-Based Composites", *Acta Metallurgica*, Vol. 40, No. 6, 1992, pp. 1201-1222.
13. S. K. Mannan and John deBarbadillo, "Long Term Thermal Stability of INCONEL alloy 783", Paper Presented at the International Gas Turbine & Aeroengine Congress & Exhibition, Stockholm, Sweden, June 2-5, pp. 1-10.
14. L. Z. Ma, K. M. Chang, S. K. Mannan, S. J. Patel, "Effect of Isothermal Exposure on Elevated-Temperature, Time-Dependent Fatigue-Crack Propagation in INCONEL alloy 783", *Metallurgical Transactions*, Vol. 33A, 2002, pp. 3465-3478.
15. R. F. Decker, "Strengthening Mechanisms in Nickel-Base Superalloys", Paper presented at Steel Strengthening Mechanisms Symposium, Zurich, Switzerland, May 5-6, 1969, pp. 1-24.
16. E. A. Fell, "The effect of Thermal Treatment on the Constitution of 80-20 Nickel-Chromium Alloys Hardened with Titanium and Aluminum", *Metallurgica*, Vol. 63, 1961, pp. 157-166
17. G. N. Maniar and J. E. Bridge Jr., "Effect of Gamma-Gamma Prime Mismatch, Volume Fraction Gamma Prime, and Gamma Prime Morphology on Elevated Temperature Properties of Ni, 20Cr, 5.5Mo, Ti, Al Alloys", *Metallurgical Transactions*, 1970, Vol. 2, pp. 95-102.

